Since January 2020 Elsevier has created a COVID-19 resource centre with free information in English and Mandarin on the novel coronavirus COVID-19. The COVID-19 resource centre is hosted on Elsevier Connect, the company's public news and information website.

Journal of Molecular Graphics and Modelling 114 (2022) 108201

Contents lists available at ScienceDirect

Journal of Molecular Graphics and Modelling

journal homepage: www.elsevier.com/locate/jmgm

Inhibitory mechanism of Ambroxol and Bromhexine Hydrochlorides as potent blockers of molecular interaction between SARS-CoV-2 spike protein and human angiotensin-converting Enzyme-2

Idowu A. Kehinde *, Anu Egbejimi, Manvir Kaur, Collins Onyenaka, Tolulope Adebusuyi, Omonike A. Olaleye

Department of Pharmaceutical and Environmental Health Sciences, College of Pharmacy and Health Sciences, Texas Southern University, 3100 Cleburne St, Houston, TX, 77004, USA

ARTICLE INFO

Keywords:
SARS-CoV-2
hACE-2
Ambroxol hydrochlorides
Bromhexine hydrochlorides
Molecular interaction
Computational techniques

ABSTRACT

Severe acute respiratory syndrome coronavirus 2 (SARS-CoV-2) infects the host cells through interaction of its spike protein with human angiotensin-converting enzyme 2 (hACE-2). High binding affinity between the viral spike protein and host cells hACE-2 receptor has been reported to enhance the viral infection. Thus, the disruption of this molecular interaction will lead to reduction in viral infectivity. This study, therefore, aimed to analyze the inhibitory potentials of two mucolytic drugs; Ambroxol hydrochlorides (AMB) and Bromhexine hydrochlorides (BHH), to serve as potent blockers of these molecular interactions and alters the binding affinity/efficiency between the proteins employing computational techniques. The study examined the effects of binding of each drug at the receptor binding domain (RBD) of the spike protein and the exopeptidase site of hACE-2 on the binding affinity (ΔG_{bind}) and molecular interactions between the two proteins. Binding affinity revealed that the binding of the two drugs at the RBD-ACE-2 site does not alter the binding affinity and molecular interaction between the proteins. However, the binding of AMB (−56.931 kcal/mol) and BHH (−46.354 kcal/mol) at the exopeptidase site of hACE-2, significantly reduced the binding affinities between the proteins compared to the unbound, ACE-2-RBD complex (−64.856 kcal/mol). The result further showed the two compounds have good affinity at the hACE-2 site, inferring they might be potent inhibitors of hACE-2. Residue interaction networks analysis further revealed the binding of the two drugs at the exopeptidase site of hACE-2 reduced the number of interacting amino residues, subsequently leading to loss of interactions between the two proteins, with BHH showing better reduction in the molecular interaction and binding affinity than AMB. The result of the structural analyses additionally, revealed that the binding of the drugs considerably influences the dynamic of the complexes when compared to the unbound complex. The findings from this study suggest the binding of the two drugs at the exopeptidase site reduces the binding effectiveness of the proteins than their binding at the RBD site, and consequently might inhibit viral attachment and entry.

1. Introduction

Coronavirus disease 2019 (COVID-19) is the current and most dangerous pandemic the world has ever experienced. As of April 11, 2022, approximately 500 million cases and over 6 million deaths have been confirmed and reported worldwide (https://coronavirus.jhu.edu/map.html). Severe acute respiratory syndrome coronavirus 2 (SAR-CoV-2) is the causative agent of the disease [37]. SAR-CoV-2 is a member of a class of enveloped and positive-sense RNA viruses, belonging to the Coronaviridae family [24]. The SAR-CoV-2 are spherical in shape, consisting of four major structural proteins; spike, envelope, nucleocapsid and membrane proteins.

The spike protein is the most crucial protein that controls essential biological processes which include attachment, fusion and viral entry in the host cell. Following the fusion of the virus with the host cell membrane through the spike protein, the viral genomic particles (RNA) are released into the host cells, making use of the host cells machinery to produce numerous viral copies capable of reinfecting other cells. A vital

* Corresponding author.
E-mail address: kehinde.idowu@tsu.edu (I.A. Kehinde).

https://doi.org/10.1016/j.jmgm.2022.108201
Received 5 September 2021; Received in revised form 11 April 2022; Accepted 12 April 2022
Available online 21 April 2022
1093-3263/Published by Elsevier Inc.

process in the virus entry is the interaction between the virus spike protein and receptor proteins on the surface of the host cells, known as human angiotensin-converting enzyme 2 (hACE-2). hACE-2 is a metalloenzyme (zinc-containing enzyme) found on the membrane surface of different cells such as the intestinal enterocytes, kidney cells, duodenum, and more cells [6,9,12,33]. The protein has two different domains namely, an N-terminal (peptidase M2) domain and a C-terminal (collectrin renal amino acid transporter) domain [12].

The receptor protein (hACE2) has been reported to serves as the main entry point into host cells by coronaviruses such as HCoV-NL63, SARS-CoV-1 and 2 [7,21–23,38,40,43].https://en.wikipedia.org/wiki/Angiotensin-converting_enzyme_2 - cite_note-29 Fusion and translocation of SARS-CoV-1 and 2 specifically result from the binding of the virus spike S1 protein to the hACE-2 enzymatic domain on host cells surface [26,34]. This binding resulted in the formation of crucial and much needed RBD-hACE-2 complex which enhance viral entry [39].

Studies have also shown there is high affinity for interaction between SARS-CoV-2 spike protein and hACE-2 than SARS-CoV-1 spike protein and hACE-2 [3,13,35,39]. Basu et al., further reported that SARS-CoV-2 spike protein showed between 10 and 20 times binding affinity to hACE-1 than SARS-CoV-1 [3]. Studies have shown the development or identification of therapeutics that can lower or affect the binding affinity/efficiency of spike proteins to its receptor, hACE-2, will be a significant step to inhibit SARS-CoV-2 attachment, and subsequently prevent infections [20,36].

It is therefore essential to identify small molecules that can influence the binding efficiency of spike protein with hACE-2 receptor, and possibly act as inhibitor of the virus attachment. In this study, we employed computational techniques to analyze the inhibitory potentials of Ambroxol Hydrochlorides (AMB) and Bromhexine Hydrochlorides (BHH) to serve as potent blockers of these molecular interactions between the viral spike proteins and hACE-2 receptor. The study examined the effects of binding of each drug at the RBD site of the spike protein and exopeptidase site of hACE-2 on the binding affinity and molecular interactions between the two proteins.

Ambroxol Hydrochlorides (AMB) and Bromhexine Hydrochlorides (BHH) are referred to as mucolytic drugs, used for the treatment of respiratory diseases such as common colds, cystic fibrosis, chronic bronchitis, chronic obstructive pulmonary diseases and many more [1]. Both drugs have been repurposed as potent inhibitors of SARS-CoV-2. No doubt, their usage as therapeutic agents against respiratory diseases has prompted studies to examine their antiviral potentials against SARS-CoV-2. Currently three or more clinical trials are on-going to test their effectiveness against covid-19 (NCT04355026, NCT04273763, NCT04340349) (Hörnich et al., 20201). BHH has been reported to inhibit TMPRSS2, while AMB was reported to inhibit hACE-2 [25]; https://www.bioworld.com/articles/433289-chinese-biotechs-apply-new-tech-to-accelerate-drug-rd-for-covid-19). Another recent study revealed that BHH reduced TMPRSS2-activated cell-cell fusion by SARS-CoV-1 and SARS-CoV-2 spike proteins [14]. A Clinical study further showed that treatment with BHH relieved lung injury, without severe adverse effects, and clinically effective against COVID-19 [25]. The inhibitory activities of these drugs might be attributed to their inhibition of host cells receptors required by SARS-CoV-2 attachment and entry for infection.

2. Methods

2.1. Molecular docking and simulation

2.1.1. Protein (hACE2-RBD) acquisition and preparation

The X-ray crystal structures of the complex of SARS-CoV-2 RBD with hACE-2 (PDB code: 6LZG) was obtained from the RSCB Protein Data Bank (Wang et al., 2020). The protein structure was then prepared on the UCSF Chimera software package [41]. The structures of the protein were prepared by removing water molecules, nonstandard naming, protein residue connectivity. The two mucolytic drugs (AMB and BHH) were accessed from PubChem [19]. The 3-D structures of the drugs were prepared on the Avogadro software package [10].

2.1.2. Molecular docking

Autodock available on Chimera was used for molecular docking [32], with default docking parameters. Before docking, Gasteiger charges were added to the drug molecules, and the non-polar hydrogen atoms were merged to carbon atoms. The molecules were then docked first into the hACE-2 catalytic binding pocket, and secondly, at the hACE-2-RBD binding site by defining the grid box with a spacing of 1 Å each and size and (22 × 18 × 22) and (32 × 41 × 25) pointing in x, y and z directions, respectively. The best docking poses for the two drugs were then subjected to molecular dynamics simulations.

2.1.3. Molecular dynamic (MD) simulations

The MD simulation was performed as described by Idowu et al. [15,16]. The simulations were performed using the GPU version provided with the AMBER package (AMBER 18), in which the FF18SB variant of the AMBER force field [27] was used to describe the systems.

ANTECHAMBER was used to generate atomic partial charges for the ligand by utilizing the Restrained Electrostatic Potential (RESP) and the General Amber Force Field (GAFF) procedures. The Leap module of AMBER 18 allowed for the addition of hydrogen atoms and, Naˆ+ counter ions to ACE2-RBD complex to neutralize all systems. The systems were then suspended implicitly within an orthorhombic box of TIP3P water molecules such that all atoms were within 10 Å of any box edge [18].

An initial minimization of 2000 steps were carried out with an applied restraint potential of 500 kcal/mol for both solutes. They were performed for 1000 steps using the steepest descent method followed by 1000 steps of conjugate gradients. An additional full minimization of 1000 steps were further carried out using the conjugate gradient algorithm without restraint. A gradual heating MD simulation from 0 K to 300 K was executed for 50 ps, such that the systems maintained a fixed number of atoms and fixed volume. The systems' solutes were imposed with a potential harmonic restraint of 10 kcal/mol and collision frequency of 1.0 ps. Following heating, an equilibration estimating 500 ps of each system was conducted; the operating temperature was kept constant at 300 K. Additional features such as several atoms and pressure were also held constant, mimicking an isobaric-isothermal ensemble. The system's pressure was maintained at 1 bar using the Berendsen barostat [2,8].

The total time for the MD simulations conducted was 100 ns. In each simulation, the SHAKE algorithm was employed to constrict hydrogen atoms' bonds [29]. The step size of each simulation was 2fs, and an SPFP precision model was used. The simulations coincided with the isobaric-isothermal ensemble (NPT), with randomized seeding, the constant pressure of 1 bar maintained by the Berendsen barostat [2], a pressure-coupling constant of 2 ps, a temperature of 300 K and Langevin thermostat [17] with a collision frequency of 1.0 ps.

2.1.4. Post-dynamic analysis

Analysis of Root Means Square Deviation (RMSD), Radius of Gyration (Rg), and Solvent Accessible Surface Area (SASA) was done using the CPPTRAJ module employed in the AMBER 18 suit. All raw data plots were generated using the Origin data analysis software [30].

2.1.5. Binding free energy calculations

To estimate and compare the systems' binding affinity, the free binding energy was calculated using the Molecular Mechanics/GB Surface Area method (MM/GBSA) [42]. Binding free energy was averaged over 100000 snapshots extracted from the 100 ns trajectory. The free binding energy (ΔG) computed by this method for each molecular species (complex, ligand, and receptor) can be represented as:

$$\Delta G_{bind} = G_{complex} - G_{receptor} - G_{ligand} \quad (1)$$

$$\Delta G_{bind} = E_{gas} + G_{sol} - TS \quad (2)$$

$$E_{gas} = E_{int} + E_{vdw} + E_{ele} \quad (3)$$

$$G_{sol} = G_{GB} + G_{SA} \quad (4)$$

$$G_{SA} = \gamma SASA \quad (5)$$

E_{gas} denotes the gas-phase energy, which consists of the internal energy E_{int}, Coulomb energy E_{ele} and the van der Waals energies E_{vdw}. The E_{gas} was directly estimated from the FF14SB force field terms. Solvation free energy, G_{sol}, was estimated from the energy contribution from the polar states, G_{GB}, and non-polar states, G. The non-polar solvation energy, SA. G_{SA} was determined from the solvent-accessible surface area (SASA), using a water probe radius of 1.4 Å. In contrast, the polar solvation, G_{GB}, the contribution was estimated by solving the GB equation. S and T denote the total entropy of the solute and temperature, respectively.

3. Results and discussion

Studies have shown that molecular interactions between SARS-CoV-2 spike glycoprotein (SARS-CoV-2 S_{pg}) and human angiotensin-converting enzyme 2 (hACE-2) is an essential mechanism required for the entry of SARS-CoV-2 virus into the host cell [4,5,39]. Studies further suggests that there is high affinity for interaction between SARS-CoV-2 S_{pg} and hACE-2 to form the much-needed RBD-ACE-2 complex required for viral entry, and this high binding affinity, is one of the major elements enhancing the rapid spread of the disease [13,35,39]. Therefore, the development or identification of therapeutics that can lower the binding affinity or inhibit the molecular interactions between the two proteins will help in lowering the spread of the disease.

In this study, the inhibitory potentials of Ambroxol and Bromhexine Hydrochlorides to serve as potent blockers of these molecular interactions between the two proteins were examined using computational techniques. The study examined the effects of binding of each drug at the RBD site of the spike protein and exopeptidase site of hACE-2 on the binding affinity and molecular interactions between the two proteins. Molecular mechanics/generalised born surface area (MMGBSA) computational technique was used to calculate the binding energies (ΔG_{bind}) between the two proteins. Table 1 showed the binding affinity between the two proteins before and after the drugs bind at the RBD site of Spike protein. In the absence of any of the drugs (unbound complex), the result revealed a high binding energy of −64.856 kcal/mol between the two proteins. In another study by Calcagnile et al. a higher binding energy of 48.150 kcal/mol was reported between hACE-2 and SARS-CoV-2 spike protein [5]. In this study, the binding of AMB and BHH at the Spike protein RBD showed no difference in the binding energies between the two proteins (AMB, -62.442 kcal/mol and BHH, −60.323 kcal/mol) when compared with the control. This result, therefore, suggests the binding of the two drugs at the spike RBD does not affect the binding affinity and molecular interaction between the two proteins. A further investigation of the binding energy of the two drugs at the RBD site of spike protein revealed the drugs have relatively low binding energies at the spike RBD site (Table 2). This might explain the insignificant effects the two drugs exhibited on the binding affinities of the two proteins.

Furthermore, the study examined the impacts of binding of the drugs at the exopeptidase site of hACE-2 on the binding affinity and molecular interactions between the two proteins. As shown in Table 3, the binding of the two drugs showed significant reduction in the binding energies between the two proteins.

with BHH showing better reduction of −46.354 kcal/mol compared with AMB and the control with binding energies of −56.931 kcal/mol and −64.856 kcal/mol, respectively. A similar molecular docking study reported Hesperidin alters the binding energy of bound complex of ACE2 and spike protein [3]. This result suggests that the binding of the two drugs at the exopeptidase site of hACE-2 lowers the binding affinity between the two proteins and might possibly discourage the formation of RBD-ACE-2 complex required for viral entry. This result corroborates existing studies that reported both AMB and BHH inhibit hACE-2, and clinically effective against COVID-19 [14,25], and might explain the mechanism. This encouraging result further prompt the investigation of the binding energy of the two drugs at the exopeptidase site of hACE-2 (Table 4). The results showed that the two drugs have higher binding energies at the exopeptidase site of the hACE-2, however, BHH binds better with hACE-2 than AMB. This result of this study therefore suggests that the better the binding of the drugs at the exopeptidase site of hACE-2 the lower the binding affinity between the two proteins. This thereby justifies the significant reduction in binding affinity recorded for BHH in Table 3.

Tables 5 and 6 showed the summaries of the amino acid residues interactions and the types of interactions (such as hydrogen bond, p-p stacked interaction, and van der Waals (vdW) overlaps) observed between the proteins, respectively. As shown in Table 5, ACE-2-RBD complex (unbound) has a total of thirty-two amino acid residues interactions between the two proteins (16 amino acids each from each proteins). The binding of AMB to the complex has a total of thirty-one amino acids interaction between the two proteins, with thirteen amino acid residues from hACE-2 interacting with Eighteen amino acid residues from the spike protein. While the binding of BHH to the complex at the exopeptidase site lowers the total number of amino interactions to twenty-seven, with twelve amino residues from hACE-2 and fifteen residues from the spike protein. The binding of BHH at the exopeptidase site exhibits more inhibitory effects than AMB.

Furthermore, Table 6 showed there are 13 hydrogen bonds, 15 Vander Waal forces and 3 pi-Pi stack interactions in the ACE-2-RBD (unbound) complex. However, the binding of AMB resulted to loss of Vander Waal interactions between Gln6 of the hACE-2 and Ala740 of the Spike protein. Another van der Waals interaction loss was also observed between Leu61 (from ACE-2) and Phe751 of the spike protein. Two

Table 1
Thermodynamic Binding Free Energy Profiles for the Spike RBD towards hACE2 before and after ligands binding at RBD-hACE2.

Energy Components (kcal/mol)					
Complex	Δ E_{vdW}	ΔE_{elec}	ΔG_{gas}	ΔG_{solv}	ΔG_{bind}
Spike RBD					
hACE-2	−97.115 ± 7.209	−633.804 ± 32.284	−730.920 ± 33.671	666.063 ± 30.008	−64.856 ± 10.190
hACE-2 (AMB)	−101.185 ± 6.210	−640.138 ± 37.294	−741.324 ± 37.294	676.881 ± 36.207	−62.442 ± 8.084
hACE-2 (BHH)	−105.249 ± 8.143	−644.924 ± 42.126	−750.173 ± 8.449	672.850 ± 40.818	−60.323 ± 3.054

ΔEele electrostatic energy, ΔEvdW van der Waals energy, ΔGbind total binding free energy, ΔGsol solvation free energy, ΔEgas gas-phase free energy.

Table 2
Thermodynamic Binding Free Energy Profiles for the ligands at the hACE2-Spike RBD site.

Energy Components (kcal/mol)					
Complex	Δ E_{vdW}	ΔE_{elec}	ΔG_{gas}	ΔG_{solv}	ΔG_{bind}
Spike RBD					
AMB	−18.857 ± 3.788	−198.962 ± 15.770	−211.817 ± 17.351	198.136 ± 17.351	−24.681 ± 4.668
BHH	−23.063 ± 3.332	−206.210 ± 18.233	−221.271 ± 16.841	189.810 ± 16.285	−37.032 ± 3.054

ΔEele electrostatic energy, ΔEvdW van der Waals energy, ΔGbind total binding free energy, ΔGsol solvation free energy, ΔEgas gas-phase free energy.

Table 3
Thermodynamic Binding Free Energy Profiles for the Spike RBD towards hACE2 before and after ligands binding at Exopeptidase site of hACE-2.

Energy Components (kcal/mol)					
Complex	**Δ E_{vdW}**	**ΔE_{elec}**	**ΔG_{gas}**	**ΔG_{solv}**	**ΔG_{bind}**
Spike RBD					
hACE-2	−97.115 ± 7.209	−633.804 ± 32.284	−730.920 ± 33.671	666.063 ± 30.008	−64.856 ± 10.190
hACE-2 (AMB)	−99.732 ± 5.779	−601.075 ± 57.201	−700.808 ± 57.174	641.877 ± 54.576	−56.931 ± 7.897
hACE-2 (BHH)	−95.045 ± 5.660	−609.859 ± 50.001	−704.905 ± 50.868	658.550 ± 47.230	−46.354 ± 8.191

Table 4
Thermodynamic Binding Free Energy Profiles for the ligands at the hACE2 binding site of hACE2-Spike RBD.

Energy Components (kcal/mol)					
Complex	**Δ E_{vdW}**	**ΔE_{elec}**	**ΔG_{gas}**	**ΔG_{solv}**	**ΔG_{bind}**
hACE-2					
AMB	−31.797 ± 7.254	−195.455 ± 6.282	−214.784 ± 19.098	177.787 ± 7.899	−42.231 ± 5.324
BHH	−40.063 ± 3.332	−188.320 ± 10.122	−206.424 ± 11.232	189.810 ± 8.245	−54.032 ± 7.158

ΔEele electrostatic energy, ΔEvdW van der Waals energy, ΔGbind total binding free energy, ΔGsol solvation free energy, ΔEgas gas-phase free energy.

Table 5
Interacting Amio residues before and after ligands binding at hACE-2 Exopeptidase site.

Complex	Interacting amino acids of hACE-2 receptor	Interacting amino acids of Spike protein
hACE-2-RBD	Ser1, Gln6, Thr9, Phe10, Lys13, His16, Glu17, Glu19, Asp20, Tyr23, Leu61, Met64, Tyr65, Lys335, Asp337, Asn376	Tyr714, Tyr718, Leu720, Phe721, Tyr738, Ala740, Phe751, Asn752, Tyr754, Phe755, Gln758, Gln763, Thr765, Tyr766, Gly767, Tyr770,
hACE-2-RBD-AMB	Ser1, Gln6, Thr9, Phe10, Lys13, His16, Glu17, Glu19, Tyr23, Met64, Tyr65, Lys335, Asp337	Tyr718, Leu720, Phe721, Tyr738, Ala740, Phe751, Asn752, Tyr754, Phe755, Leu757, Gln758, Tyr760, Tyr761, Gln763, Thr765, Asn766, Gly767, Tyr770
hACE-2-RBD-BHH	Gln6, Thr9, Phe10, Lys12, Lys13, His16, Glu19, Leu61, Met64, Tyr65, Lys335, Asp337	Tyr718, Leu720, Phe721, Tyr738, Ala740, Phe751, Asn752, Tyr754, Phe755, Leu757, Gln758, Thr765, Tyr766, Gly767, Tyr770,

additional hydrogen bonds (Asp20-Tyr714 and Asn376-Tyr770) were loss after the binding of AMB when compared with the unbound, RBD-ACE-2 complex. The binding of BHH, however, led to more loss of molecular interactions between the proteins, which justified the lower binding affinity recorded between the two proteins. Three Hbonds were lost between Ser1-Ala740, Asp20-Tyr714 and Asn376-Tyr770. In addition, two van der Waals forces were lost, between Glu17-Gln758 and Tyr23-Gln763. A strong Pi-Pi stack interaction was also lost between residues Phe10 and Tyr754. The binding of the BHH at the exopeptidase site prevent molecular interactions, subsequently decreasing the binding affinity between the proteins (see Fig. 1).

Investigating the molecular stability, the effects of binding of the drugs to the RBD-ACE-2 complex were assessed by the evaluation of the Root Means Square Deviation (RMSD), Radius of Gyration (RoG), and Solvent Accessible Surface Area (SASA) values of alpha carbon (Ca) atoms of the complexes from the entire molecular dynamics' trajectory

Table 6
Summary of Residues interaction networks (RINs) and interaction types.

Residues hACE-2 Spike	Δ E_{vdW}	ΔE_{elec}	ΔG_{gas}
Ser1 – Ala740	Hbond	Hbond	
Gln6 - Ala740	Vdw	–	Vdw
Gln6 - Asn752	Hbond, Vdw	Hbond, Vdw	Hbond, Vdw
Thr9 – Phe721	Vdw	Vdw	Vdw
Thr9 - Tyr738	Vdw	Vdw	Vdw
Phe10 - Tyr754	Pi-pi Stack, Vdw	Pi-pi Stack, Vdw	Hbond, Vdw
Lys12 - Phe721	–	–	Vdw
Lys13 - Leu720	Vdw	Vdw	Vdw
Lys13 - Phe 755	Hbond	Hbond, Vdw	Hbond
Lys13 - Leu 757	Hbond	Hbond	Hbond
Lys13 - Gln 758	Hbond	Hbond, Vdw	Hbond
His16 - Tyr718	Pi-pi Stack	Pi-pi Stack, Vdw	Pi-pi Stack
His16 - Leu720	Vdw	Vdw	Vdw
His16 - Gln 758	Vdw	Vdw	Vdw
Glu17 - Gln 758	Vdw	Vdw	–
Glu19 - Tyr770	Hbond	Hbond, Vdw	Hbond
Asp20 - Tyr714	Hbond	–	–
Tyr23 - Gln763	Vdw	Vdw	–
Tyr23 - Thr 765	–	Hbond	–
Tyr23 - Asn 766	–	Hbond, Vdw	–
Leu61 - Phe751	Vdw	–	Vdw
Met64 - Phe 751	Vdw	Vdw	Vdw
Tyr65 - Phe 751	Pi-Pi Stack, Vdw	Pi-Pi Stack, Vdw	Pi-Pi Stack, Vdw
Tyr65 - Asn 752	Hbond	Hbond, Vdw	Hbond
Tyr65 - Tyr754	Hbond	Hbond	Hbond
Lys335 - Tyr760	–	Hbond	–
Lys335 - Tyr761	–	Hbond	–
Lys335 - Tyr766	Hbond, Vdw	Hbond, Vdw	Hbond, Vdw
Lys335 - Gly767	Hbond	Hbond	Hbond
Lys335 - Tyr770	Vdw	Hbond	Vdw
Asp337 - Thr 765	Hbond	Hbond, Vdw	Hbond
Asn376 - Tyr770	Hbond	–	–

(Fig. 2a–c). Studies have shown that binding of molecules to specific target are usually accompanied or resulted to conformational changes that might affect the activity of the target [16,28,31]. Fig. 2a showed the result of the RMSD plot that measures the complexes' convergence and stability. A lower RMSD value indicates a more stable complex [11]. The plot revealed the average RMSD values for the bound (ACE-2-RBD-AMB and ACE-2-RBD-BHH) and unbound (ACE-2-RBD) complexes are low, inferring that the hACE-2-RBD complexes are stability.

The average RMSD values of the complexes after AMB (2.713 Å) and BHH (2.441 Å) binds to the exopeptidase site of hACE-2 are relatively higher than the average value for the unbounded control (1.971 Å). The result revealed that the binding of the drugs considerably influences the dynamic of the complex when compared to the unbound complex. To further quantify the effects of the drugs' binding on the exposure of the complexes to solvent environments, the SASA values were also estimated. From the result of Fig. 2b, the average SASA values for ACE-2-RBD, ACE-2-RBD-AMB and ACE-2-RBD-BHH complexes are 34.530 Å, 33.140 Å and 32.960 Å. respectively. The result showed a slight decrease in the exposure of the bound complexes to solvent molecules, which indicated that their binding to the complex slightly affect the structural dynamic of the complexes, but the structural integrity of the complexes is not compromised. The RoG plots of the bound complexes showed slight increase compared to the unbound complex (Fig. 2c). The average RoG values for the unbound complex is 30.541 $Å^2$, while the average values for ACE-2-RBD-AMB and ACE-2-RBD-BHH complexes are 31.279 $Å^2$ and 30.809 $Å^2$ respectively. This indicates the overall structural compactness of the bound complexes are slightly differs to the unbound complex. The structural analyses, therefore revealed that the binding of the drugs considerably influences the dynamic of the complexes when compared to the unbound complex.

4. Conclusion

In conclusion, this study supports the existing finding which report

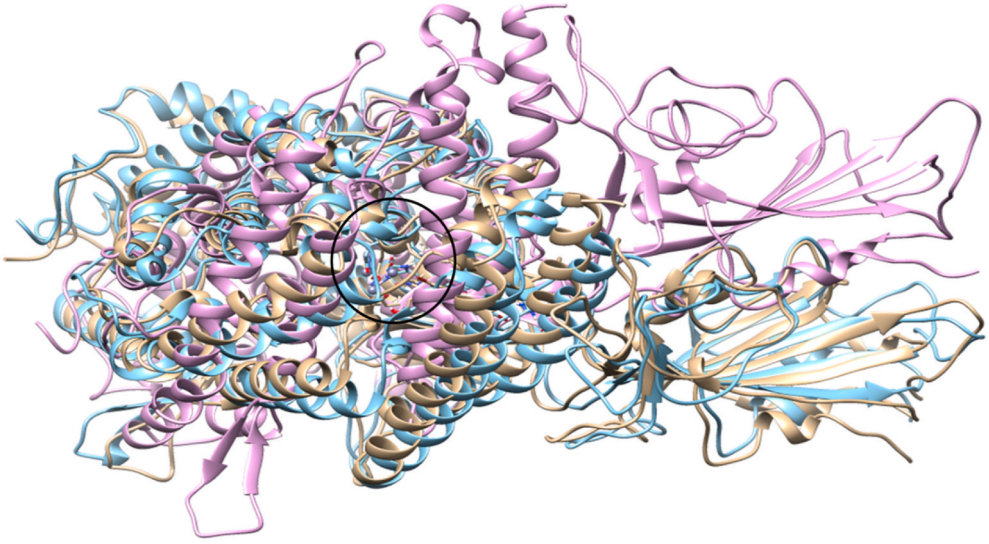

Fig. 1. Superimpositions of the snapshot structures of ligand-hACE2-RBD complexes of AMB (in brown), BHH *(in cyan) and Apo-Complex (in magenta). AMB in red and BHH in deep blue at the exopeptidase site of hACE-2.*

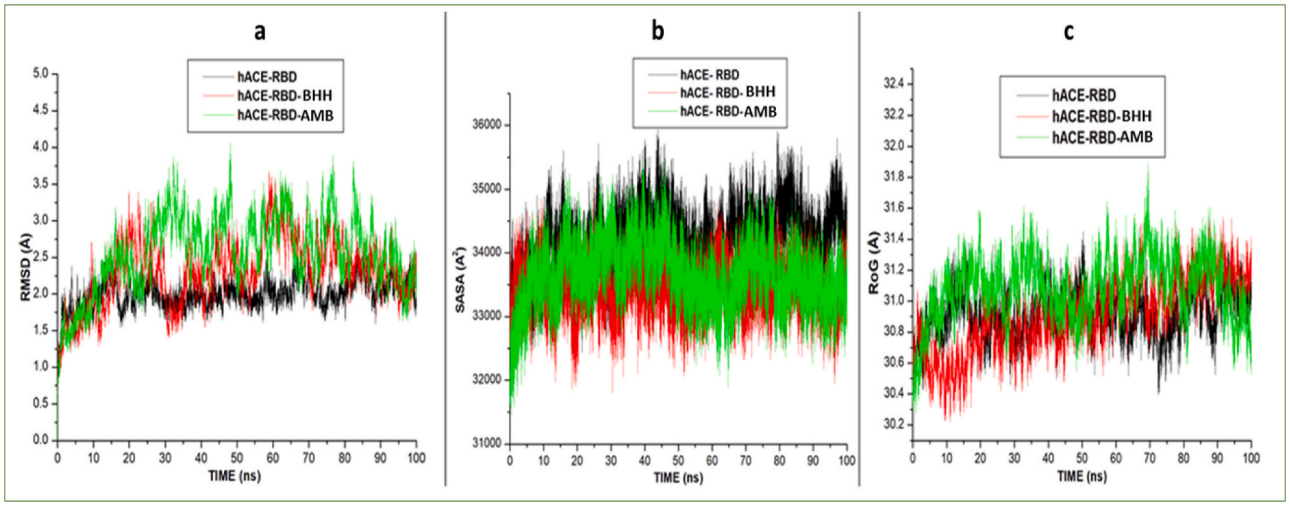

Fig. 2. Comparative a). RMSD b). SASA, and c). RoG profile plots of C-a atoms of BHH and AMB ligands at the hACE2 exopeptidase site of hACE2-RBD calculated throughout 100 ns molecular dynamics simulation.

that high binding affinity exists between the hACE-2 and SARS-CoV-2 spike protein, as evidenced in the high binding energy recorded between the two proteins. The study further revealed that the binding of the two drugs at the exopeptidase site of hACE-2 significantly alters molecular interactions and lower binding effectiveness between the two proteins than their binding at the RBD site. This study, therefore, suggests both AMB and BHH might be good inhibitor of hACE-2, reduce binding affinity between spike protein and hACE-2, and consequently inhibit viral attachment, entry, and infectivity.

Funding source

This project is sponsored by the NIH-RCMI (U54MD007605) and CPRIT-CTTP (RP210043) Grants.

Declaration of competing interest

The authors declare that they have no known competing financial interests or personal relationships that could have appeared to influence the work reported in this paper.

References

[1] S.D. Aaron, Mucolytics for COPD: negotiating a slippery slope towards proof of efficacy, Eur. Respir. J. 50 (4) (2017), https://doi.org/10.1183/13993003.01465-2017, 2017.

[2] J.E. Basconi, M.R. Shirts, Effects of temperature control algorithms on transport properties and kinetics in molecular dynamics simulations, J. Chem. Theor. Comput. 9 (7) (2013) 2887–2899, https://doi.org/10.1021/ct400109a.

[3] A. Basu, A. Sarkar, U. Maulik, Molecular docking study of potential phytochemicals and their effects on the complex of SARS-CoV2 spike protein and human ACE2, Sci. Rep. 10 (2020) 17699, https://doi.org/10.1038/s41598-020-74715-4, 2020.

[4] M. Bosso, T.A. Thanaraj, M. Abu-Farha, M. Alanbaei, J. Abubaker, F. Al-Mulla, The two faces of ACE2: the role of ACE2 receptor and its polymorphisms in hypertension and COVID-19, Mol. Ther. Methods Clin. Dev. 18 (2020) 321e327, https://doi.org/10.1016/2Fj.omtm.2020.06.017, 2020.

[5] M. Calcagnile, P. Forgez, A. Iannelli, C. Bucci, M. Alifano, P. Alifano, ACE2 polymorphisms and individual susceptibility to SARS-CoV-2 infection: insights from an in silico study, bioRxiv 4 (23) (2020), 057042, https://doi.org/10.1101/2020.04.23.057042.

[6] M. Donoghue, F. Hsieh, E. Baronas, K. Godbout, M. Gosselin, N. Stagliano, M. Donovan, B. Woolf, K. Robison, R. Jeyaseelan, R.E. Breitbart, S. Acton, A novel angiotensin-converting enzyme–related carboxypeptidase (ACE2) converts angiotensin I to angiotensin 1-9, Circ. Res. 87 (5) (2000) e1–e9, https://doi.org/10.1161/01.RES.87.5.e1.

[7] A.R. Fehr, S. Perlman, Coronaviruses: an overview of their replication and pathogenesis, Coronaviruses. Methods in Molecul. Biol. 1282 (2015) 1–23, https://doi.org/10.1007/978-1-4939-2438-7_1. Springer New York, 978-1-4939-2437-0.
[8] P. Gonnet, P-SHAKE: a quadratically convergent SHAKE in O(n2), J. Comput. Phys. 220 (2) (2007) 740–750, https://doi.org/10.1016/j.jcp.2006.05.032.
[9] I. Hamming, W. Timens, M.L. Bulthuis, A.T. Lely, G. Navis, H. van Goor, Tissue distribution of ACE2 protein, the functional receptor for SARS coronavirus. A first step in understanding SARS pathogenesis, J. Pathol. 203 (2) (2004) 631–637, https://doi.org/10.1002/path.1570.
[10] M.D. Hanwell, D.E. Curtis, D.C. Lonie, T. Vandermeerschd, E. Zurek, G. R. Hutchison, Avogadro: an advanced semantic chemical editor, visualization, and analysis platform, J. Cheminf. 4 (8) (2012) 1–17.
[11] B. Hess, Convergence of sampling in protein simulations, Phys. Rev. 65 (3) (2002) 31910.
[12] F. Hikmet, L. Méar, Å. Edvinsson, P. Micke, M. Uhlén, C. Lindskog, The protein expression profile of ACE2 in human tissues, Mol. Syst. Biol. 16 (7) (2020), https://doi.org/10.15252/msb.20209610.
[13] M. Hoffmann, H. Kleine-Weber, S. Pöhlmann, SARS-CoV-2 cell entry depends on ACE2 and TMPRSS2 and is blocked by a clinically proven protease inhibitor, Cell 181 (2020) 271–280, e8.
[14] B.F. Hörnich, A.K. Großkopf, S. Schlagowski, M. Tenbusch, H. Kleine-Weber, F. Neipel, C. StahlHennig, A.S. Hahn, SARS-CoV-2 and SARS-CoV spike-mediated cell-cell fusion differ in their requirements for receptor expression and proteolytic activation, e00002-21, J. Virol. 95 (2021), https://doi.org/10.1128/JVI.00002-21, https://www.bioworld.com/articles/433289-chinese-biotechs-apply-new-tech-to-accelerate-drug-rd-for-covid-19.
[15] I. Kehinde, P. Ramharack, M. Nlooto, M. Gordon, The pharmacokinetic properties of HIV-1 protease inhibitors: a computational perspective on herbal phytochemicals, Heliyon 5 (10) (2019), e02565, https://doi.org/10.1016/j.heliyon.2019.e02565.
[16] K. Idowu, P. Ramharack, M. Nlooto, M. Gordon, Molecular dynamic mechanism(s) of inhibition of bioactive antiviral phytochemical compounds targeting cytochrome P450 3A4 and P-glycoprotein, J. Biomol. Struct. Dynam. (2020) 1–11, https://doi.org/10.1080/07391102.2020.1821780.
[17] J.A. Izaguirre, D.P. Catarello, J.M. Wozniak, R.D. Skeel, Langevin stabilization of molecular dynamics, J. Chem. Phys. 114 (5) (2001) 2090–2098, https://doi.org/10.1063/1.1332996.
[18] W.L. Jorgensen, J. Chandrasekhar, J.D. Madura, R.W. Impey, M.L. Klein, Comparison of simple potential functions for simulating liquid water, J. Chem. Phys. 79 (2) (1983) 926–935.
[19] S. Kim, P.A. Thiessen, E.E. Bolton, J. Chen, G. Fu, A. Gindulyte, L. Han, J. He, S. He, B.A. Shoemaker, J. Wang, B. Yu, J. Zhang, S.H. Bryant, PubChem substance and compound databases, Nucleic Acids Res. 44 (D1) (2016) D1202–D1213.
[20] Khan A, Waris H, Rafique M, Suleman M, Mohammad A, Ali SS, Khan T, Waheed Y, Liao C, Wei DQ. The Omicron (B.1.1.529) variant of SARS-CoV-2 binds to the hACE2 receptor more strongly and escapes the antibody response: insights from structural and simulation data. Int. J. Biol. Macromol.. 1;200:438-448. doi: 10.1016/j.ijbiomac.2022.01.059.
[21] K. Kuba, Y. Imai, S. Rao, H. Gao, F. Guo, B. Guan, A crucial role of angiotensin converting enzyme 2 (ACE2) in SARS coronavirus-induced lung injury, Nat. Med. 11 (8) (2005) 875–879, https://doi.org/10.1038/nm1267.
[22] R. Lewis, COVID-19 vaccine will close in on the spikes. DNA science blog. Public library of science, Archived from the original on 2020-02-22 (2020). Retrieved 2020-02-22.
[23] F. Li, Receptor recognition and cross-species infections of SARS coronavirus, Antivir. Res. 100 (1) (2013), https://doi.org/10.1016/j.antiviral.2013.08.014, 246–54.
[24] G. Lippi, F. Sanchis-Gomar, B.M. Henry, COVID-19: unravelling the clinical progression of nature's virtually perfect biological weapon, Ann. Transl. Med. 8 (2020) 693, https://doi.org/10.21037/2Fatm-20-3989.
[25] D. Markus, L. Gottfried, M. Markus, R. Marina, B. Dario, V. Danielle de, A SARS-CoV-2 prophylactic and treatment; A counter argument against the sole use of chloroquine 8 (4) (2020), https://doi.org/10.34297/AJBSR.2020.08.001283. AJBSR.MS.ID.001283.
[26] J.K. Millet, G.R. Whittaker, Physiological and molecular triggers for SARS-CoV membrane fusion and entry into host cells, Virol. 517 (2018) 3–8, https://doi.org/10.1016/j.virol.2017.12.015.
[27] P.C. Nair, J.O. Miners, Molecular dynamics simulations: from structure function relationships to drug discovery, in: Silico Pharm vol. 2, 2014, pp. 1–4, https://doi.org/10.1186/s40203-014-0004-8, 1.
[28] P. Ramharack, S. Oguntade, M.E.S. Soliman, Delving into Zika virus structural dynamics – a closer look at NS3 helicase loop flexibility and its role in drug discovery, RSC Adv. 7 (36) (2017) 22133–22144, https://doi.org/10.1039/C7RA01376K.
[29] J.P. Ryckaert, G. Ciccotti, H.J. Berendsen, Numerical integration of the Cartesian equations of motion of a system with constraints: molecular dynamics of n-alkanes, J. Comput. Phys. 23 (3) (1977) 327–341, https://doi.org/10.1016/0021-9991(77)90098-5.
[30] E. Seifert, OriginPro 9.1: scientific data analysis and graphing software-software review, J. Chem. Inf. Model. 54 (5) (2014), 1552–1552.
[31] T. Sindhu, P. Srinivasan, Exploring the binding properties of agonists interacting with human TGR5 using structural modeling, molecular docking and dynamics simulations, RSC Adv. 5 (19) (2015) 14202–14213.
[32] O. Trott, A.J. Olson, AutoDock vina: improving the speed and accuracy of docking with a new scoring function, efficient optimization, and multithreading, J. Comput. Chem. 31 (2010) 455–461.
[33] A.J. Turner, ACE2 cell biology, regulation, and physiological functions, in: T. Unger, M. Ulrike, U.M. Steckelings, R.A. dos Santos (Eds.), The Protective Arm of the Renin Angiotensin System (RAS): Functional Aspects and Therapeutic Implications, Academic Press, 2015, ISBN 978-0-12-801364-9, pp. 185–189, https://doi.org/10.1016/B978-0-12-801364-9.00025-0 (Chapter 25).
[34] H. Wang, P. Yang, K. Liu, F. Guo, Y. Zhang, G. Zhang, C. Jiang, SARS coronavirus entry into host cells through a novel clathrin- and caveolae-independent endocytic pathway, Cell Res. 18 (2) (2008) 290–301, https://doi.org/10.1038/cr.2008.15.
[35] Q. Wang, Y. Zhang, L. Wu, S. Niu, C. Song, Z. Zhang, G. Lu, C. Qiao, Y. Hu, K. Y. Yuen, Q. Wang, H. Zhou, J. Yan, J. Qi, Structural and functional basis of SARS-CoV-2 entry by using human ACE2, Cell 181 (2020) 894–904, e9.
[36] C. Wang, S. Wang, D. Li, D.Q. Wei, J. Zhao, J. Wang, Human intestinal defensin 5 inhibits SARS-CoV-2 invasion by cloaking ACE2, Gastroenterology 159 (3) (2020) 1145–1147, https://doi.org/10.1053/j.gastro.2020.05.015, e4.
[37] World Health Organization, Director-General's opening remarks at the media, *Briefing on COVID-19* [WWW Document]. URL, https://www.who.int/dg/speech, 2020.
[38] World Health Organization, What are the official names of the disease and the virus that causes it? Q&A on coronaviruses (2020). Archived from the original on 5 March 2020. Retrieved 22 February 2020.
[39] N. Wrapp, K.S. Wang, J.A. Corbett, C.L. Goldsmith, O. Hsieh, B.S. Abiona, J. S. Graham, A. McLellan, Cryo-EM structure of the 2019-nCoV spike in the prefusion conformation, Science 367 (6483) (2020) 1260e1263, https://doi.org/10.1126/science.abb2507.
[40] X. Xu, P. Chen, J. Wang, J. Feng, H. Zhou, X. Li, Evolution of the novel coronavirus from the ongoing Wuhan outbreak and modeling of its spike protein for risk of human transmission, Sci. China Life Sci. 63 (3) (2020) 457–460, https://doi.org/10.1007/s11427-020-1637-5.
[41] Z. Yang, K. Lasker, D. Schneidman-Duhovny, B. Webb, C.C. Huang, E.F. Pettersen, T.D. Goddard, E.C. Meng, A. Sali, T.E. Ferrin, UCSF chimera, MODELLER, and IMP: an integrated modeling system, J. Struct. Biol. 179 (3) (2012) 269–278.
[42] M. Ylilauri, O.T. Pentikɛainen, MMGBSA as a tool to understand the binding affinities of filamin-peptide interactions, J. Chem. Inf. Model. 53 (10) (2013) 2626–2633.
[43] P. Zhou, X.L. Yang, X.G. Wang, B. Hu, L. Zhang, W. Zhang, A pneumonia outbreak associated with a new coronavirus of probable bat origin, Nature 579 (7798) (2020) 270–273, https://doi.org/10.1038/s41586-020-2012-7.